

Sphalerons in the NMSSM

Koichi Funakubo^{a,1}, Akira Kakuto^{b,2} Shuichiro Tao^{a,3} and Fumihiko Toyoda^{b,4}

^{a)}*Department of Physics, Saga University, Saga 840-8502 Japan*

^{b)}*School of Humanity-Oriented Science and Engineering, Kinki University, Iizuka 820-8555 Japan*

Abstract

We study sphaleron solutions in the next-to-minimal supersymmetric standard model. We find that the boundary condition on the singlet field at the origin of the radial coordinate is of Neumann type, while the other boundary conditions are of Dirichlet type. The sphaleron energy takes almost the same value as in the MSSM for wide range of parameters, in spite of the negative contribution from the cubic term in the Higgs potential.

1 Introduction

Since the discovery of the sphaleron solution[1], unsuppressed transition of the baryon number at high temperatures has been recognized to play an important role in early universe. It yielded new possibilities of matter generation, baryogenesis through leptogenesis and electroweak baryogenesis[2]. The latter requires that the sphaleron process decouples just after the electroweak phase transition, in order to protect the generated baryon asymmetry from washout by sphaleron process in equilibrium. This sphaleron decoupling condition is expressed as $\Gamma_{\text{sph}}(T) \simeq T e^{-E_{\text{sph}}/T} < H(T)$, where E_{sph} is the static energy of the sphaleron solution and $H(T)$ is the Hubble parameter at temperature T . In the standard model with one Higgs doublet, this condition can be cast into the form of $v_C/T_C > 1$, where v_C is the expectation value of the Higgs field at the transition temperature T_C , where the gauge symmetry is spontaneously broken. Thus, the knowledge of energy of the sphaleron solution in a model viable for electroweak baryogenesis is indispensable to qualify the model by examining the sphaleron decoupling condition. The sphaleron solution was originally found in the 4-dimensional $SU(2)$ gauge theory

¹e-mail: funakubo@cc.saga-u.ac.jp

²e-mail: kakuto@fuk.kindai.ac.jp

³e-mail: tao@higgs.phys.kyushu-u.ac.jp

⁴e-mail: ftoyoda@fuk.kindai.ac.jp

with one Higgs doublet[3]. The minimal standard model, however, cannot afford to generate the baryon asymmetry at the electroweak phase transition with an acceptable Higgs mass. It was also pointed out that the CP violation in the KM matrix is insufficient to provide the chiral charge as the source of baryon number. Hence, one must extend the standard model for successful electroweak baryogenesis. In particular, models with more bosonic fields are expected to admit the strongly first-order phase transition. Among those models are the MSSM with a light stop and the two-Higgs-doublet model. The sphaleron solutions have been found in the two-Higgs-doublet model[4] and in the MSSM with finite-temperature corrections[5]. The model with one Higgs doublet and one singlet is among those extensions of the standard model for which a sphaleron solution has been found[6].

We recently found that the Next-to-MSSM (NMSSM), which contains a singlet superfield in addition to the MSSM, can have strongly first-order phase transition, with heavy stops and Higgs bosons whose masses and couplings are consistent with results of collider experiments so far[7]. Although the NMSSM has more parameters than the MSSM, there are more constraints on these parameters which are absent in the MSSM. For example, the electroweak vacuum is not always the absolute minimum of the Higgs potential. This is because the cubic terms containing the singlet scalar can easily generate minimum of the potential other than the electroweak vacuum. We observed that the vacuum condition, which ensures that the electroweak vacuum be the absolute minimum of the effective potential, together with the spectrum condition on the Higgs scalars, restricts allowed parameters in the model[8]. In order to determine the parameter sets which are suited for the baryogenesis, one must know the sphaleron solution and its energy in this model. In the MSSM-limit, where the vacuum expectation value of the singlet goes to infinity, the sphaleron solutions are expected to have the same profile as the MSSM. When the expectation value is of order of the weak scale, we expect new features of the phase transitions, but even the existence of the sphaleron solution is not obvious. Our aim is to find the sphaleron solution and to study its energy in the case of weak-scale expectation value of the singlet field.

Since the sphaleron solution is a saddle-point configuration, it is difficult to find it by solving the full equations of motion. Instead, we usually adopt the ansatz including the parameter along the noncontractible loop in the configuration space[3]. The ansatz is constructed in such a way that the configuration corresponds to the vacuum at the loop parameter $\mu = 0$ and π , while the configuration at $\mu = \pi/2$ is expected to be the highest-energy one corresponding to the sphaleron. In order to ensure that the configuration is the sphaleron, one must check that the configuration does satisfy the full equation of motion and that the fluctuation spectrum around the configuration does contain only one negative mode. In practice, these procedure are complicated and has been done only in the one-doublet model[9]. Here we extend the ansatz including the noncontractible loop to the NMSSM with $U(1)$ -gauge sector being turned off, and write down the static spherically symmetric equations of motion for the configuration at $\mu = \pi/2$. Then we

solve the equations of motion and evaluate the energy along the noncontractible loop around the solution to ensure that it is the highest-energy configuration along the loop.

This paper is organized as follows. In §2, we extend the ansatz of Klinkhammer and Manton for the configurations along the noncontractible loop to the NMSSM. Then we derive the equations of motion for the sphaleron configurations. Several numerical solutions for the equations are shown in §3 for parameter sets corresponding to the light-Higgs and the heavy-Higgs scenarios. Section 4 is dedicated to concluding remarks. The derivation of the asymptotic solutions, together with the boundary conditions, are summarized in the Appendix.

2 Ansatz and equations of motion

2.1 noncontractible loop

As discussed in [1], any static configuration of finite-energy doublet scalar $\Phi(\mathbf{x})$ defines a map from S^2 spanned by the spatial coordinates (θ, ϕ) to $S^3 = SU(2)$ which characterizes the field at $r = \infty$ as a unitary transformation of the vacuum $\begin{pmatrix} 0 \\ 1 \end{pmatrix}$. A one-parameter family of such configurations connecting vacua, which cannot be contracted to a point, is constructed by realizing the family of maps as a map from S^3 to S^3 . Among such one-parameter families, that of the highest symmetry is expected to form the least energy set of configurations. The configuration with the highest energy along the parameter will be a saddle-point configuration with one negative mode.

The Manton's ansatz for the noncontractible loop in the one-doublet model is

$$\Phi(\mu, r, \theta, \phi) = \frac{v}{\sqrt{2}} \left\{ (1 - h(r)) \begin{pmatrix} 0 \\ e^{-i\mu} \cos \mu \end{pmatrix} + h(r) U(\mu, \theta, \phi) \begin{pmatrix} 0 \\ 1 \end{pmatrix} \right\}, \quad (2.1)$$

$$A_i(\mu, r, \theta, \phi) = -\frac{i}{g} f(r) \partial_i U(\mu, \theta, \phi) U^{-1}(\mu, \theta, \phi), \quad (2.2)$$

where

$$U(\mu, \theta, \phi) = \begin{pmatrix} e^{i\mu}(\cos \mu - i \sin \mu \cos \theta) & e^{i\phi} \sin \mu \sin \theta \\ -e^{-i\phi} \sin \mu \sin \theta & e^{-i\mu}(\cos \mu + i \sin \mu \cos \theta) \end{pmatrix}. \quad (2.3)$$

Here $\mu \in [0, \pi]$ and the configurations are reduced to the vacuum at $\mu = 0$ and π . As for the NMSSM, we adopt the following ansatz for the doublet Higgs fields, Φ_d and Φ_u , and the singlet n ,

$$\begin{aligned} \Phi_d(\mu, r, \theta, \phi) &= \frac{v_d}{\sqrt{2}} \left\{ (1 - h_1(r)) \begin{pmatrix} e^{i\mu} \cos \mu \\ 0 \end{pmatrix} + h_1(r) U(\mu, \theta, \phi) \begin{pmatrix} 1 \\ 0 \end{pmatrix} \right\} \\ &= \frac{v_d}{\sqrt{2}} \begin{pmatrix} e^{i\mu}(\cos \mu - i h_1(r) \sin \mu \cos \theta) \\ -e^{-i\phi} h_1(r) \sin \mu \sin \theta \end{pmatrix}, \\ \Phi_u(\mu, r, \theta, \phi) &= \frac{v_u e^{i\rho}}{\sqrt{2}} \left\{ (1 - h_2(r)) \begin{pmatrix} 0 \\ e^{-i\mu} \cos \mu \end{pmatrix} + h_2(r) U(\mu, \theta, \phi) \begin{pmatrix} 0 \\ 1 \end{pmatrix} \right\} \end{aligned} \quad (2.4)$$

$$= \frac{v_u e^{i\rho}}{\sqrt{2}} \left(e^{i\phi} h_2(r) \sin \mu \sin \theta \right. \\ \left. e^{-i\mu} (\cos \mu + i h_2(r) \sin \mu \cos \theta) \right), \quad (2.5)$$

$$n(\mu, r, \theta, \phi) = \frac{v_n e^{i\varphi}}{\sqrt{2}} k(r). \quad (2.6)$$

Now the profile functions to be solved are $f(r)$, $h_1(r)$, $h_2(r)$ and $k(r)$.

The lagrangian of the gauge-Higgs sector of the NMSSM is given by

$$\mathcal{L} = -\frac{1}{4} F_{\mu\nu}^a F^{a\mu\nu} + (D_\mu \Phi_d)^\dagger D^\mu \Phi_d + (D_\mu \Phi_u)^\dagger D^\mu \Phi_u + \partial_\mu n^* \partial^\mu n - V_0(\Phi_d, \Phi_u, n), \quad (2.7)$$

where the Higgs potential is given by

$$V_0(\Phi_d, \Phi_u, n) = m_1^2 \Phi_d^\dagger \Phi_d + m_2^2 \Phi_u^\dagger \Phi_u + m_N^2 |n|^2 - \left(\lambda A_\lambda n \Phi_d \Phi_u + \frac{\kappa}{3} A_\kappa n^3 + \text{h.c.} \right) \\ + \frac{g_2^2 + g_1^2}{8} (\Phi_d^\dagger \Phi_d - \Phi_u^\dagger \Phi_u)^2 + \frac{g_2^2}{2} |\Phi_d^\dagger \Phi_u|^2 \\ + |\lambda|^2 |n|^2 (\Phi_d^\dagger \Phi_d + \Phi_u^\dagger \Phi_u) + |\lambda \Phi_d \Phi_u + \kappa n^2|^2, \quad (2.8)$$

The terms in the first line of (2.8) are the soft supersymmetry-breaking terms, those in the second line comes from the D -term potential, which are the same as those in the MSSM, and those in the last line are the F -terms, which are peculiar to the NMSSM. Here we adopt the same notation as in [8].

All the parameters in the potential with mass dimensions are to be determined once one specifies the breaking mechanism of the supersymmetry and the mass scale relevant to it. Instead of specifying supersymmetry-breaking mechanism, we express them in terms of the vacuum expectation values (VEVs) of the Higgs fields by requiring that the tree-level potential has vanishing first derivatives at the prescribed vacuum parametrized by the VEV of the doublet v_0 , the ratio of the doublet VEVs $\tan \beta$ and the VEV of the singlet v_n . As shown in [8]⁵, the derivatives of V_0 with respect to the CP-even order parameters vanish at the vacuum, if the soft masses are given by

$$m_1^2 = \left(R_\lambda - \frac{1}{2} \mathcal{R} v_n \right) v_n \tan \beta - \frac{1}{2} m_W^2 \cos(2\beta) - \frac{|\lambda|^2}{2} (v_0^2 \sin^2 \beta + v_n^2), \quad (2.9)$$

$$m_2^2 = \left(R_\lambda - \frac{1}{2} \mathcal{R} v_n \right) v_n \cot \beta + \frac{1}{2} m_W^2 \cos(2\beta) - \frac{|\lambda|^2}{2} (v_0^2 \cos^2 \beta + v_n^2), \quad (2.10)$$

$$m_N^2 = (R_\lambda - \mathcal{R} v_n) \frac{v_0^2}{v_n} \sin \beta \cos \beta + R_\kappa v_n - \frac{|\lambda|^2}{2} v^2 - |\kappa|^2 v_n^2, \quad (2.11)$$

while those with respect to the CP-odd order parameters vanish, if

$$I_\lambda = \frac{1}{2} \mathcal{I} v_n. \quad (2.12)$$

⁵Since we are working with $g_1 = 0$, we should set $m_Z = m_W$ in the results in [8].

Here we defined the following parameters which are independent of phase convention,

$$\begin{aligned}
R_\lambda &= \frac{1}{\sqrt{2}} \operatorname{Re} \left(\lambda A_\lambda e^{i(\rho+\varphi)} \right), & I_\lambda &= \frac{1}{\sqrt{2}} \operatorname{Im} \left(\lambda A_\lambda e^{i(\rho+\varphi)} \right), \\
R_\kappa &= \frac{1}{\sqrt{2}} \operatorname{Re} \left(\kappa A_\kappa e^{3i\varphi} \right), \\
\mathcal{R} &= \operatorname{Re} \left(\lambda \kappa^* e^{i(\rho-2\varphi)} \right), & \mathcal{I} &= \operatorname{Im} \left(\lambda \kappa^* e^{i(\rho-2\varphi)} \right).
\end{aligned} \tag{2.13}$$

We use these relations to express the static energy functional which is

$$E[\Phi_d, \Phi_u, n] = \int d^3 \mathbf{x} \left[\frac{1}{4} F_{ij}^a F_{ij}^a + (D_i \Phi_d)^\dagger D_i \Phi_d + (D_i \Phi_u)^\dagger D_i \Phi_u + |\partial_i n|^2 + V_0(\Phi_d, \Phi_u, n) \right], \tag{2.14}$$

in terms of the profile functions. Upon inserting the ansatz for the noncontractible loop, (2.1), (2.2), (2.4), (2.5) and (2.6), into (2.14), we obtain

$$\begin{aligned}
&E[f, h_1, h_2, k](\mu) \\
&= \frac{4\pi v_0}{g_2} \int_0^\infty d\xi \left\{ 4 \sin^2 \mu \left[(f')^2 + \frac{2f^2(1-f)^2}{\xi^2} \sin^2 \mu \right] \right. \\
&\quad + \frac{\cos^2 \beta \sin^2 \mu}{2} \left[\xi^2 (h_1')^2 + 2(h_1^2(1-f)^2 + (1-h_1)^2 f^2 \cos^2 \mu \right. \\
&\quad \quad \left. \left. - 2h_1(1-h_1)f(1-f) \cos^2 \mu \right) \right] \\
&\quad + \frac{\sin^2 \beta \sin^2 \mu}{2} \left[\xi^2 (h_2')^2 + 2(h_2^2(1-f)^2 + (1-h_2)^2 f^2 \cos^2 \mu \right. \\
&\quad \quad \left. \left. - 2h_2(1-h_2)f(1-f) \cos^2 \mu \right) \right] + \frac{N^2 \xi^2}{2} (k')^2 \\
&\quad + \frac{A}{8} \xi^2 \sin^2 \beta \cos^2 \beta \left[(h_1^2 + h_2^2 - 2k(h_1 h_2 - 1) - 2) \sin^2 \mu + (k-1)^2 \right] \\
&\quad + \frac{C_{\mathcal{R}} N^2 \xi^2}{4} \sin \beta \cos \beta \left[2k(k-1)(h_1 h_2 - 1) \sin^2 \mu + (k-1)^2 \right] \\
&\quad + \frac{\xi^2}{32} [(h_1^2 - 1) \cos^2 \beta - (h_2^2 - 1) \sin^2 \beta]^2 \sin^4 \mu \\
&\quad + \frac{\xi^2}{12} \sin^2 \beta \cos^2 \beta \sin^2 \mu \cos^2 \mu (h_1 - h_2)^2 \\
&\quad + \frac{C_\lambda \xi^2}{4} \sin^2 \beta \cos^2 \beta \sin^2 \mu \left[(h_1 h_2 - 1)^2 \sin^2 \mu - \frac{1}{3} (h_1 - h_2)^2 (2 + \sin^2 \mu) \right] \\
&\quad + \frac{C_\lambda N^2 \xi^2}{4} (k^2 - 1) \left[(h_1^2 - 1) \cos^2 \beta + (h_2^2 - 1) \sin^2 \beta \right] \sin^2 \mu \\
&\quad \left. + \frac{C_\kappa N^4 \xi^2}{4} (k^2 - 1)^2 - \frac{BN^2 \xi^2}{6} (2k^3 - 3k^2 + 1) \right\} \\
&= \frac{4\pi v_0}{g_2} \left(c_2 \sin^4 \mu + c_1 \sin^2 \mu + c_0 \right), \tag{2.15}
\end{aligned}$$

where $\xi = g_2 v_0 r$ and the primes on the profile functions denote the derivatives with respect

to ξ . We introduced dimensionless parameters defined by

$$\begin{aligned}
A &= \frac{(R_\lambda - \mathcal{R}v_n/2)v_n}{m_W^2 \sin \beta \cos \beta} = \frac{\hat{m}^2}{m_W^2} = \frac{4}{g_2^2 v_0^2} \left(m_{H^\pm}^2 - m_W^2 + \frac{\lambda^2}{2} v_0^2 \right), \\
N &= \frac{v_n}{v_0}, \quad B = \frac{R_\kappa N}{g_2^2 v_0}, \\
C_{\mathcal{R}} &= \frac{\mathcal{R}}{g_2^2}, \quad C_\lambda = \frac{|\lambda|^2}{g_2^2}, \quad C_\kappa = \frac{|\kappa|^2}{g_2^2},
\end{aligned} \tag{2.16}$$

and the coefficients in the last expressions are defined by

$$\begin{aligned}
c_2 &= \int_0^\infty d\xi \left[\frac{8f^2(1-f)^2}{\xi^2} - \cos^2 \beta f(1-h_1)(f-2h_1+fh_1) - \sin^2 \beta f(1-h_2)(f-2h_2+fh_2) \right. \\
&\quad + \frac{\xi^2}{32} \left((h_1^2-1) \cos^2 \beta - (h_2^2-1) \sin^2 \beta \right)^2 - \frac{\xi^2}{12} \sin^2 \beta \cos^2 \beta (h_1-h_2)^2 \\
&\quad \left. + \frac{C_\lambda \xi^2}{4} \sin^2 \beta \cos^2 \beta \left((h_1 h_2 - 1)^2 - \frac{1}{3} (h_1 - h_2)^2 \right) \right], \tag{2.17}
\end{aligned}$$

$$\begin{aligned}
c_1 &= \int_0^\infty d\xi \left[4(f')^2 + \frac{\cos^2 \beta}{2} (\xi^2 (h_1')^2 + 2(h_1 - f)^2) + \frac{\sin^2 \beta}{2} (\xi^2 (h_2')^2 + 2(h_2 - f)^2) \right. \\
&\quad + \frac{A}{8} \xi^2 \sin^2 \beta \cos^2 \beta (h_1^2 + h_2^2 - 2k(h_1 h_2 - 1) - 2) \\
&\quad + \frac{C_{\mathcal{R}} N^2 \xi^2}{2} \sin \beta \cos \beta k(k-1)(h_1 h_2 - 1) + \frac{1-2C_\lambda}{12} \xi^2 \sin^2 \beta \cos^2 \beta (h_1 - h_2)^2 \\
&\quad \left. + \frac{C_\lambda N^2 \xi^2}{4} (k^2 - 1) \left((h_1^2 - 1) \cos^2 \beta + (h_2^2 - 1) \sin^2 \beta \right) \right], \tag{2.18}
\end{aligned}$$

$$\begin{aligned}
c_0 &= \int_0^\infty d\xi \xi^2 \left[\frac{N^2}{2} (k')^2 + \frac{A}{8} \sin^2 \beta \cos^2 (k-1)^2 + \frac{C_{\mathcal{R}} N^2}{4} \sin \beta \cos \beta (k-1)^2 \right. \\
&\quad \left. + \frac{C_\kappa N^4}{4} (k^2 - 1)^2 - \frac{BN^2}{6} (2k^3 - 3k^2 + 1) \right]. \tag{2.19}
\end{aligned}$$

In the presence of the CP violation, the \mathcal{I} -dependent term in the potential is proportional to $\sin \mu \cos \mu \cos \theta$, which vanishes upon integration over θ to yield the static energy of the configuration. This might suggest that an ansatz without spherical symmetry reduces the potential energy compared to the spherically symmetric one in the CP-violating case, but such an ansatz with less symmetry will increase the gradient energy. Hence we expect that the spherically symmetric ansatz yields the least energy configuration for each μ , as long as the CP violation is not so large.

The equations of motion for the sphaleron are derived by applying the variational method to the energy functional (2.15) with $\mu = \pi/2$. After solving the equations, we check that the configuration is at least locally maximum at $\mu = \pi/2$ along the noncontractible loop by calculating the coefficients c_2 and c_1 . That is, the coefficients calculated with the solution must satisfy $2c_1 + c_2 > 0$, for which $E''(\mu = \pi/2) < 0$.

2.2 equations of motion

The static energy functional at $\mu = \pi/2$ is given by

$$\begin{aligned}
& E[f, h_1, h_2, k] \\
&= \frac{4\pi v_0}{g_2} \int_0^\infty d\xi \left\{ 4 \left[(f')^2 + \frac{2(f-f^2)^2}{\xi^2} \right] + \frac{N^2}{2} \xi^2 (k')^2 \right. \\
&\quad + \frac{1}{2} \cos^2 \beta \left[\xi^2 (h_1')^2 + 2(1-f)^2 h_1^2 \right] + \frac{1}{2} \sin^2 \beta \left[\xi^2 (h_2')^2 + 2(1-f)^2 h_2^2 \right] \\
&\quad + \frac{A}{8} \sin^2 \beta \cos^2 \beta \xi^2 (h_1^2 + h_2^2 + k^2 - 2h_1 h_2 k - 1) \\
&\quad + \frac{C_{\mathcal{R}} N^2}{4} \sin \beta \cos \beta \xi^2 \left(2k(k-1)h_1 h_2 - (k^2 - 1) \right) \\
&\quad + \frac{\xi^2}{32} \left[(h_1^2 - 1) \cos^2 \beta - (h_2^2 - 1) \sin^2 \beta \right]^2 \\
&\quad + \frac{C_\lambda}{4} \xi^2 \left[\sin^2 \beta \cos^2 \beta (h_1^2 - 1)(h_2^2 - 1) + N^2 (k^2 - 1)(h_1^2 \cos^2 \beta + h_2^2 \sin^2 \beta - 1) \right] \\
&\quad \left. + \frac{C_\kappa N^4}{4} \xi^2 (k^2 - 1)^2 - \frac{BN^2}{6} \xi^2 (k-1)(2k^2 - k - 1) \right\}. \tag{2.20}
\end{aligned}$$

Applying the variational method to this functional, we obtain the equations of motion for the profile functions:

$$f''(\xi) = \frac{2}{\xi^2} f(1-f)(1-2f) - \frac{1-f}{4} \left(h_1^2 \cos^2 \beta + h_2^2 \sin^2 \beta \right), \tag{2.21}$$

$$\begin{aligned}
& h_1''(\xi) + \frac{2}{\xi} h_1'(\xi) \\
&= \frac{2(1-f)^2 h_1}{\xi^2} + \frac{A}{4} \sin^2 \beta (h_1 - h_2 k) + \frac{C_{\mathcal{R}} N^2}{2} \tan \beta h_2 k (k-1) \\
&\quad + \frac{h_1}{8} \left((h_1^2 - 1) \cos^2 \beta - (h_2^2 - 1) \sin^2 \beta \right) + \frac{C_\lambda}{2} \left((h_2^2 - 1) \sin^2 \beta + N^2 (k^2 - 1) \right) h_1, \tag{2.22}
\end{aligned}$$

$$\begin{aligned}
& h_2''(\xi) + \frac{2}{\xi} h_2'(\xi) \\
&= \frac{2(1-f)^2 h_2}{\xi^2} + \frac{A}{4} \cos^2 \beta (h_2 - h_1 k) + \frac{C_{\mathcal{R}} N^2}{2} \cot \beta h_1 k (k-1) \\
&\quad - \frac{h_2}{8} \left((h_1^2 - 1) \cos^2 \beta - (h_2^2 - 1) \sin^2 \beta \right) + \frac{C_\lambda}{2} \left((h_1^2 - 1) \cos^2 \beta + N^2 (k^2 - 1) \right) h_2 \tag{2.23}
\end{aligned}$$

$$\begin{aligned}
& k''(\xi) + \frac{2}{\xi} k'(\xi) \\
&= \frac{A}{4N^2} \sin^2 \beta \cos^2 \beta (k - h_1 h_2) + \frac{C_{\mathcal{R}}}{2} \sin \beta \cos \beta (h_1 h_2 (2k - 1) - k) \\
&\quad + \frac{C_\lambda}{2} (h_1^2 \cos^2 \beta + h_2^2 \sin^2 \beta - 1) k + C_\kappa N^2 (k^2 - 1) k - Bk(k-1). \tag{2.24}
\end{aligned}$$

In order to solve these equations, we must specify the boundary conditions for the profile functions. We relegate the derivation of asymptotic behaviors of the solution to the

appendix and present only the result here. As shown in the appendix, the profile functions with finite energy functional satisfy the boundary conditions

$$f(0) = h_1(0) = h_2(0) = 0, \quad k'(0) = 0, \quad (2.25)$$

$$f(\infty) = h_1(\infty) = h_2(\infty) = k(\infty) = 1. \quad (2.26)$$

Note that only $k(\xi)$ at $\xi = 0$ must satisfy the boundary condition of Neumann type, while the others satisfy those of Dirichlet type.

3 Numerical solutions

In order to implement numerical study of the sphaleron solutions by solving the equations of motion (2.21) – (2.24) with the boundary conditions (2.25) and (2.26), we adopt the relaxation method which is suited for a boundary problem of ordinary differential equations. The NMSSM has more parameters than the MSSM, but some of the parameters are constrained by the vacuum condition and the Higgs spectrum condition[8]. The model with the weak scale expectation value of the singlet scalar exhibits new features with respect to the Higgs spectrum and the phase transitions[7], which are absent in the MSSM. In particular, there are four types of phase transitions at finite temperatures. Although the sphaleron solution which is relevant to the decoupling of the sphaleron process at the first-order electroweak phase transition is a configuration which mediates the symmetric phase and the broken phase at the transition temperature, we here study sphaleron configurations with the tree-level potential for parameters satisfying the tree-level vacuum condition.

In the case of the weak scale expectation value of the singlet scalar field, the allowed region in the parameter space is divided into two classes, one of which admits Higgs bosons lighter than 114GeV but with small couplings with the gauge bosons. We shall refer to this situation as the light-Higgs scenario. The other class of parameters yield heavy Higgs bosons satisfying the present bound on the neutral scalar. This situation is called the heavy-Higgs scenario, for which the Higgs spectrum and the phase transition are similar to those in the MSSM.

We found sphaleron solutions for wide range of the allowed parameters, as long as the smallest eigenvalue of the mass-squared matrix of the CP-even Higgs bosons is positive, that is, the vacuum is at least a local minimum of the potential. This is obvious from the asymptotic behaviors of solutions, derived in the appendix. In the heavy-Higgs scenario, the energy of the sphalerons E satisfy $1.6 \leq E/(4\pi v_0/g_2) \leq 1.9$ for wide range of $\tan \beta$ and v_n . The range of the sphaleron energy coincides with that in the MSSM. Further the energy becomes larger for larger mass of the lightest Higgs scalar. This behavior of the energy is expected from the results of the minimal standard model and those of the MSSM. As an illustration, we show the contour plots of the sphaleron energy and the mass of the lightest CP-even Higgs boson m_{S_1} for $\tan \beta = 5$, $v_n = 200\text{GeV}$, $m_{H^\pm} = 600\text{GeV}$ and

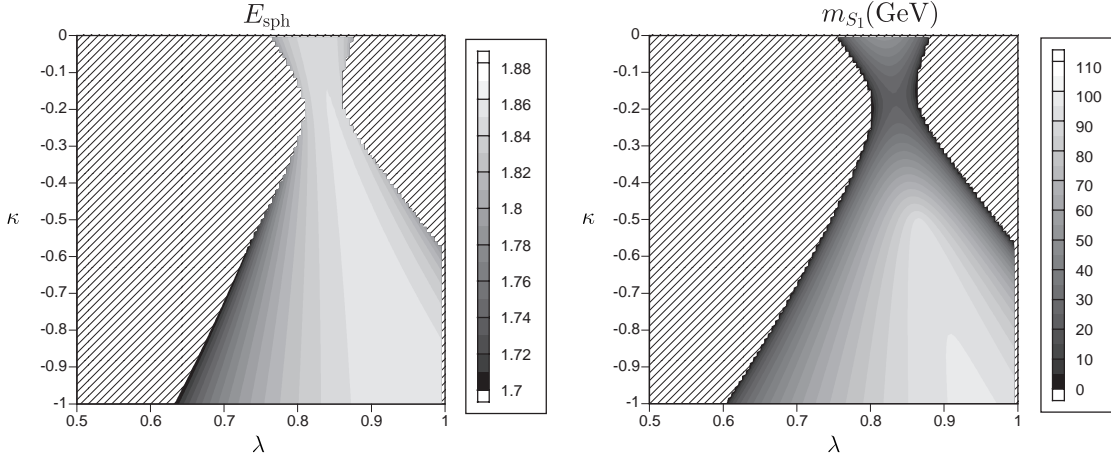


Figure 1: The sphaleron energy in the unit of $4\pi v_0/g_2$ and the mass of the lightest CP-even Higgs boson as functions of λ and κ for $\tan\beta = 5$, $v_n = 200\text{GeV}$, $m_{H^\pm} = 600\text{GeV}$ and $A_\kappa = -100\text{GeV}$.

$A_\kappa = -100\text{GeV}$ in Fig. 1. For this parameter set, both the heavy-Higgs and light-Higgs scenarios are realized for different regions in (λ, κ) -plane. Since we are working at the tree level, some of the parameter sets may be excluded by the Higgs mass bound. Our aim, however, is a qualitative study of the sphaleron solutions for a broad range of parameters. The shaded regions in Fig. 1, in which the smallest eigenvalue of the mass-squared matrix of the CP-even Higgs bosons is negative, indicates the parameters for which there is no sphaleron solution. We found that all the solutions satisfy the condition $2c_2 + c_1 > 0$, which is necessary for them to be locally maxima along the noncontractible loop in the configuration space. These contour plots show that the sphaleron energy is larger for the larger mass of the lightest Higgs scalar in the heavy-Higgs regime ($\kappa \lesssim -0.5$).

In the light-Higgs scenario ($-0.4 \lesssim \kappa \leq 0$), which is realized for small $|\kappa|$, there is a minimum of the potential along the v_n -axis. This minimum corresponds to the intermediate phase at finite temperature, at which the electroweak gauge symmetry is restored. Now we denote the potential in the symmetric phase ($v = 0$) as $U_0(k)$ defined by $U_0(k) = V_0(0, 0, v_n k/\sqrt{2})/N^2$, that is,

$$U_0(k) = \frac{C_\kappa N^2}{4} k^4 - \frac{B}{3} k^3 + \frac{1}{8} \left(\frac{A}{4N^2} - C_{\mathcal{R}} - 2C_\lambda - 4C_\kappa N^2 + 4B \right) k^2. \quad (3.1)$$

Depending on the parameters in the potential, $U_0(k)$ has a nontrivial minimum at $k \neq 0$. For smaller $|\kappa|$, the value of k at the minimum becomes larger and the value of the potential at the minimum becomes smaller. Although the parameters which yield deeper potential at the minimum than the prescribed vacuum are excluded by the vacuum condition, some of the allowed parameters admit the new type of two-stage phase transition, which is referred to as type B phase transition in [7]. As seen from Fig. 1, the sphaleron energy is not so small in spite of the small mass of the lightest Higgs scalar, in contrast to the heavy-Higgs scenario. This small enhancement of the sphaleron energy is caused by the

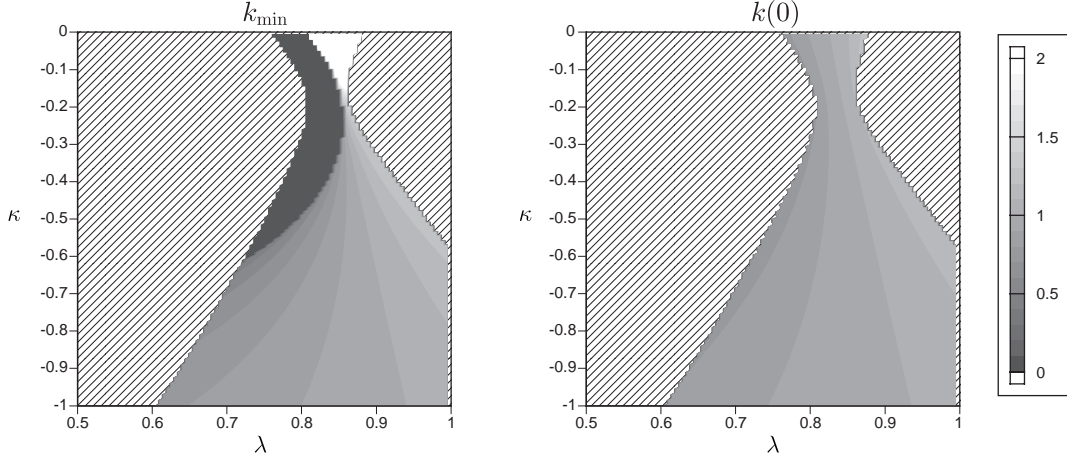


Figure 2: Contour plots of the location of the minimum of $U_0(k)$, k_{\min} , and the value of $k(0)$ of numerical solutions for the same parameter as those in Fig. 1.

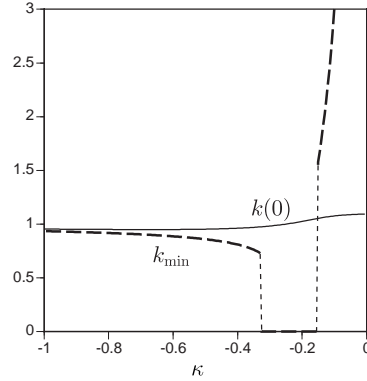


Figure 3: The values of k_{\min} and $k(0)$ along the line of $\lambda = 0.85$ in Fig. 2.

discrepancy of the boundary value $k(0)$ and the location of the minimum of the potential along the v_n -axis. In Fig. 2, we show the values of k_{\min} at which $U_0(k)$ is minimum and $k(0)$ of numerical solutions in the (λ, κ) -plane. The difference between $k(0)$ and k_{\min} is allowed because the boundary condition on $k(\xi)$ at $\xi = 0$ is of Neumann type, but not of Dirichlet type. The cross section of the contour plot at $\lambda = 0.85$ is depicted in Fig. 3. The value of k_{\min} becomes larger than 100 for $\kappa \simeq 0$, while $k(0)$ stays at a value near unity. The profile functions for $\kappa = -0.1, -0.5$ and -1 along $\lambda = 0.85$ are shown in Fig. 4. The values of the sphaleron energy of these profiles are within $(1.84 - 1.86) \times 4\pi v_0/g_2$. For $\kappa = -0.1$, $k_{\min} \simeq 2.99$ so that the profile with $k(0)$ near this point lowers the value of the potential energy, while increases the gradient energy. Then the optimal profile which minimizes the total energy has $k(0) \simeq 1.08$. In the heavy-Higgs scenario, where $k(\xi) \simeq 1$ for $0 < \xi < \infty$, the profile is similar to that in the MSSM.

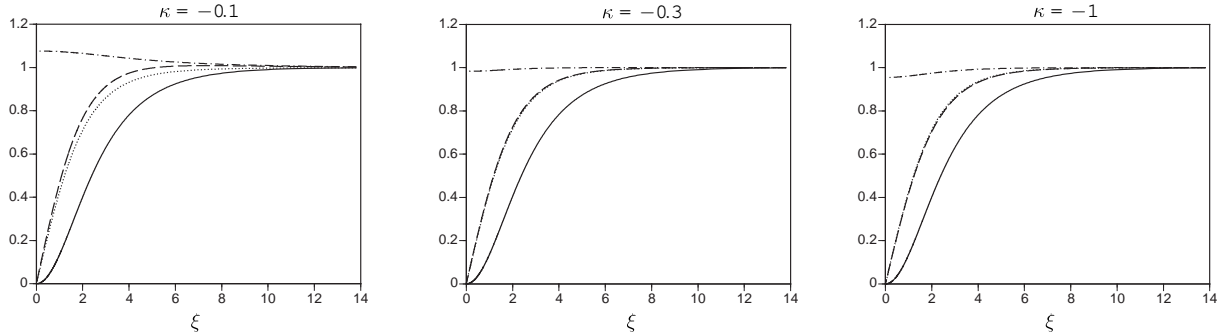


Figure 4: The profile functions $f(\xi)$ (solid curve), $h_1(\xi)$ (dashed curve), $h_2(\xi)$ (dotted curve) and $k(\xi)$ (dashed-dotted curve) for $\kappa = -0.1, -0.5$ and -1 along $\lambda = 0.85$ in Fig. 2.

4 Discussions

We have constructed the noncontractible loop in the configuration space of the NMSSM gauge-Higgs fields, from which we derived the equations of motion for the sphalerons and found a necessary condition for a solution to be a local maximum of the energy functional. We showed that the boundary condition of the singlet scalar at the origin is of Neumann type, in contrast to the other conditions of Dirichlet type. This difference in the boundary conditions in the Higgs profiles is due to the lack of gauge interaction of the singlet scalar field.

We numerically solved the equations of motion and found solutions for wide range of allowed parameters of the model. The solutions in the heavy-Higgs scenario are similar to those in the MSSM, in the sense that $k(\xi)$ stays almost constant and the energy of the solution takes the same value as that in the MSSM. The energy is larger for larger mass of the lightest Higgs scalar. This fact has been observed in the minimal standard model and in the MSSM. The sphaleron energies in the light-Higgs scenario are almost the same as those in the heavy-Higgs scenario, in spite of the small mass of the lightest Higgs scalar. This is because the difference between $k(0)$ and k_{\min} , at which the potential along $v = 0$ is the minimum, enhances the potential energy. Although the Higgs potential of the NMSSM have negative contributions from the cubic terms, the sphaleron energy in the NMSSM is almost the same as in the MSSM, for wide range of parameters. The sphaleron energy is essential to determine the sphaleron decoupling condition after the electroweak phase transition. If we assume that the prefactor in the sphaleron transition rate in the NMSSM is the same as in the MSSM, the sphaleron decoupling condition is determined solely by the energy of the sphaleron⁶. Then the sphaleron decoupling

⁶The prefactor is composed of the zero-mode contributions and the factors coming from the Gaussian integrals of the positive modes. The zero-mode contributions are mainly determined by the global symmetry of the solution, which is common to the MSSM and the NMSSM. The positive-mode contributions depend on the profile of the sphalerons. The effect of these prefactors on the transition rate is much smaller than the sphaleron energy on which the rate depends exponentially.

condition v_C/T_C , where v_C is the magnitude of the expectation value of the doublet Higgs field at the transition temperature T_C , also applies to the NMSSM.

All the numerical solutions we have found satisfy the condition $2c_2 + c_1 > 0$. As seen from the definitions of c_2 and c_1 , (2.17) and (2.18), a large negative contribution is expected to come from c_1 when $k(\xi)$ is far from unity. We could not find such solutions, but we cannot completely exclude the case of negative $2c_2 + c_1$. Even if we encounter the case of negative $2c_2 + c_1$, it may imply that our ansatz is inadequate for such parameters. In that case, we will need to know the global structure of the energy functional to decide whether the sphaleron process is possible and whether it is suppressed after the electroweak phase transition.

The sphaleron configurations obtained here are solutions with the tree-level potential. As shown in [5], the solutions with the finite-temperature effective potential differs in the energy from those with the tree-level potential by several percents in the MSSM. More precise decoupling condition of the sphaleron process in the broken phase will be obtained by solving the equations of motion with the effective potential with the radiative and finite-temperature corrections in our model.

Acknowledgements

The authors gratefully thank S. Otsuki for valuable discussions. This work was supported in part by Grant-in-Aid for Scientific Research on Priority Areas No. 13135222 to K. F. and F. T., and No. 17043009 to K. F. from the MEXT of Japan.

A Asymptotic solutions

We shall derive approximate solutions to the equations of motion for the sphaleron (2.21) – (2.24) in the asymptotic regions at $\xi \sim 0$ and $\xi \sim \infty$, respectively. For the energy functional (2.20) to have a finite value, the profile functions must behave as $f(\xi) \sim \xi^{1/2+\epsilon_f}$, $h_i(\xi) \sim \text{const.} + \xi^{-1/2+\epsilon_{h_i}}$ and $k(\xi) \sim \text{const.} + \xi^{-1/2+\epsilon_k}$ at $\xi \sim 0$. Here ϵ 's are some positive constants. Similarly, all the profile functions must approach 1 as $\xi \rightarrow \infty$. More detailed behavior of them can be obtained by the approximate equations of motion in each asymptotic region. At $\xi \sim 0$, (2.21), (2.22) and (2.23) are reduced to

$$f''(\xi) \simeq \frac{2}{\xi^2} f(\xi) - \frac{1}{4} \left(h_1^2(\xi) \cos^2 \beta + h_2^2(\xi) \sin^2 \beta \right), \quad (\text{A.1})$$

$$h_1''(\xi) + \frac{2}{\xi} h_1'(\xi) \simeq \frac{2}{\xi^2} h_1(\xi), \quad h_2''(\xi) + \frac{2}{\xi} h_2'(\xi) \simeq \frac{2}{\xi^2} h_2(\xi), \quad (\text{A.2})$$

where we have used $f(0) = 0$. The solutions to the second and third equations are $h_i(\xi) \propto \xi$ and $h_i(\xi) \propto \xi^{-2}$ for $i = 1$ and 2 , while the latter is excluded by the finiteness of the energy functional. Then (A.1) implies that $f(\xi) \propto \xi^2$, if $f(\xi)$ yield a finite energy. The asymptotic behavior of $k(\xi)$ is different from those of $h_1(\xi)$ and $h_2(\xi)$. This is because

the gauge interaction generates the dominant term proportional to $2/\xi^2$ in the right-hand sides of (A.2), whose counterpart does not exist in (2.24). In the asymptotic region $\xi \sim 0$, the equation (2.24) is approximated by

$$k''(\xi) + \frac{2}{\xi}k'(\xi) = A_0k(\xi) - Bk^2(\xi) + C_\kappa N^2 k^3(\xi), \quad (\text{A.3})$$

where we have put $A_0 = (A \sin^2 \beta \cos^2 \beta / N^2 - 2C_{\mathcal{R}} \sin \beta \cos \beta - 2C_\lambda - 4C_\kappa N^2 + 4B)/4$. In order to solve (A.3), we set

$$k(\xi) = \gamma + \sum_{n=0}^{\infty} a_n \xi^{n+\nu}, \quad (a_0 \neq 0, \nu > 0) \quad (\text{A.4})$$

where γ is some finite constant. Inserting this expression into (A.3), we obtain, to the lowest order in ξ ,

$$\nu(\nu+1)a_0\xi^{\nu-2} + (\nu+1)(\nu+2)a_1\xi^{\nu-1} + \dots = (A_0 - B\gamma + C_\kappa N^2 \gamma^2)\gamma + O(\xi^\nu). \quad (\text{A.5})$$

If $(A_0 - B\gamma + C_\kappa N^2 \gamma^2)\gamma = 0$, this equation holds only when $\nu > 2$. When $(A_0 - B\gamma + C_\kappa N^2 \gamma^2)\gamma \neq 0$, this is satisfied if $\nu = 2$ and

$$6a_0 = (A_0 - B\gamma + C_\kappa N^2 \gamma^2)\gamma, \quad a_1 = 0. \quad (\text{A.6})$$

Although γ and a_0 are not determined unambiguously at this order, it always holds that $k'(\xi = 0) = 0$. Therefore, we must impose the boundary conditions at $\xi = 0$ of Dirichlet type for $f(\xi)$, $h_1(\xi)$ and $h_2(\xi)$, and that of Neumann type for $k(\xi)$.

At $\xi \sim \infty$, all the fields must approach unity for the energy integral to be finite. To study the asymptotic behavior, we put $f(\xi) = 1 + \Delta f(\xi)$, $h_i(x) = 1 + \Delta h_i(x)$ and $k(\xi) = 1 + \Delta k(\xi)$ in the equations of motion (2.21) – (2.24) and keep only the linear terms in the deviations from 1:

$$\Delta f''(\xi) \simeq \left(\frac{1}{4} + \frac{2}{\xi^2} \right) \Delta f \simeq \frac{1}{4} \Delta f(\xi), \quad (\text{A.7})$$

$$\begin{aligned} \Delta h_1''(\xi) + \frac{2}{\xi^2} \Delta h_1'(\xi) &\simeq \frac{A}{4} \sin^2 \beta (\Delta h_1 - \Delta h_2 - \Delta k) + \frac{C_{\mathcal{R}} N^2}{2} \tan \beta \Delta k \\ &\quad + \frac{1}{4} (\Delta h_1 \cos^2 \beta - \Delta h_2 \sin^2 \beta) + C_\lambda (\Delta h_2 \sin^2 \beta + N^2 \Delta k) \\ &= \frac{A \sin^2 \beta + \cos^2 \beta}{4} \Delta h_1 + \left(-\frac{A+1}{4} + C_\lambda \right) \sin^2 \beta \Delta h_2 \\ &\quad + \left(-\frac{A}{4N^2} \sin^2 \beta + \frac{C_{\mathcal{R}}}{2} \tan \beta + C_\lambda \right) N^2 \Delta k, \end{aligned} \quad (\text{A.8})$$

$$\begin{aligned} \Delta h_2''(\xi) + \frac{2}{\xi^2} \Delta h_2'(\xi) &\simeq \frac{A}{4} \cos^2 \beta (\Delta h_2 - \Delta h_1 - \Delta k) + \frac{C_{\mathcal{R}} N^2}{2} \cot \beta \Delta k \\ &\quad - \frac{1}{4} (\Delta h_1 \cos^2 \beta - \Delta h_2 \sin^2 \beta) + C_\lambda (\Delta h_1 \cos^2 \beta + N^2 \Delta k) \end{aligned}$$

$$\begin{aligned}
&= \left(-\frac{A+1}{4} + C_\lambda \right) \cos^2 \beta \Delta h_1 + \frac{A \cos^2 \beta + \sin^2 \beta}{4} \Delta h_2 \\
&\quad + \left(-\frac{A}{4N^2} \cos^2 \beta + \frac{C_{\mathcal{R}}}{2} \cot \beta + C_\lambda \right) N^2 \Delta k, \tag{A.9}
\end{aligned}$$

$$\begin{aligned}
\Delta k''(\xi) + \frac{2}{\xi^2} \Delta k'(\xi) &\simeq \frac{A}{4N^2} \sin^2 \beta \cos^2 \beta (\Delta k - \Delta h_1 - \Delta h_2) + \frac{C_{\mathcal{R}}}{2} \sin \beta \cos \beta (\Delta h_1 + \Delta h_2 + \Delta k) \\
&\quad + C_\lambda (\Delta h_1 \cos^2 \beta + \Delta h_2 \sin^2 \beta) + 2C_\kappa N^2 \Delta k - B \Delta k \\
&= \left(-\frac{A}{4N^2} \sin^2 \beta + \frac{C_{\mathcal{R}}}{2} \tan \beta + C_\lambda \right) \cos^2 \beta \Delta h_1 \\
&\quad + \left(-\frac{A}{4N^2} \cos^2 \beta + \frac{C_{\mathcal{R}}}{2} \cot \beta + C_\lambda \right) \sin^2 \beta \Delta h_2 \\
&\quad + \left(\frac{A}{4N^2} \sin^2 \beta \cos^2 \beta + \frac{C_{\mathcal{R}}}{2} \sin \beta \cos \beta + 2C_\kappa N^2 - B \right) \Delta k. \tag{A.10}
\end{aligned}$$

Now we introduce a 3×3 symmetric matrix P whose elements are

$$\begin{aligned}
p_{11} &= \frac{1}{4} (A \sin^2 \beta + \cos^2 \beta), & p_{12} &= \left(-\frac{A+1}{4} + C_\lambda \right) \sin \beta \cos \beta, \\
p_{13} &= \left(-\frac{A}{4N^2} \sin^2 \beta + \frac{C_{\mathcal{R}}}{2} \tan \beta + C_\lambda \right) N \cos \beta, & p_{22} &= \frac{1}{4} (A \cos^2 \beta + \sin^2 \beta), \\
p_{23} &= \left(-\frac{A}{4N^2} \cos^2 \beta + \frac{C_{\mathcal{R}}}{2} \cot \beta + C_\lambda \right) N \sin \beta, \\
p_{33} &= \frac{A}{4N^2} \sin^2 \beta \cos^2 \beta + \frac{C_{\mathcal{R}}}{2} \sin \beta \cos \beta + 2C_\kappa N^2 - B. \tag{A.11}
\end{aligned}$$

The matrix P is related to the tree-level mass-squared matrix of the CP-even Higgs bosons \mathcal{M}_S^2 by $P = \mathcal{M}_S^2 / (4m_W^2)$. As long as we restrict the parameter sets to satisfy the vacuum condition, all the eigenvalues of P are positive definite. Then Eqs. (A.8) – (A.10) are written as

$$\frac{d^2}{d\xi^2} \begin{pmatrix} \Delta \tilde{h}_1(\xi) \cos \beta \\ \Delta \tilde{h}_2(\xi) \sin \beta \\ N \Delta \tilde{k}(\xi) \end{pmatrix} \simeq P \begin{pmatrix} \Delta \tilde{h}_1(\xi) \cos \beta \\ \Delta \tilde{h}_2(\xi) \sin \beta \\ N \Delta \tilde{k}(\xi) \end{pmatrix}, \tag{A.12}$$

where we have defined $\Delta \tilde{h}_i(\xi) = \xi \Delta h_i(\xi)$ and $\Delta \tilde{k}(\xi) = \xi \Delta k(\xi)$. If we denote the eigenvalue of P as λ_a , $\Delta \tilde{h}_i(\xi)$ and $\Delta \tilde{k}(\xi)$ are expressed as linear combinations of $e^{-\sqrt{\lambda_a} \xi} = e^{-m_{S_a} r}$, where m_{S_a} is the tree-level mass of the CP-even Higgs boson. Hence the asymptotic behaviors of the solutions are governed by the smallest mass of the CP-even Higgs boson.

References

- [1] N. S. Manton, Phys. Rev. **D28** (1983) 2019.
- [2] K. Funakubo, Prog. Theor. Phys. (1996) 475.
V. A. Rubakov and M. E. Shaposhnikov, Phys. Usp. **39** (1996) 461 [hep-ph/9603208].
A. Riotto and M. Trodden, Ann. Rev. Nucl. Part. Sci. **49** (1999) 35 [hep-ph/9901362].
W. Bernreuther, Lect. Notes Phys. **591** (2002) 237 [hep-ph/0205279].

- [3] F. R. Klinkhammer and N. S. Manton, Phys. Rev. **D30** (1984) 2212.
- [4] B. Kastening, R. D. Peccei and X. Zhang, Phys. Lett. **B266** (1991) 413.
- [5] J. M. Moreno, D. H. Oaknin and M. Quirós, Nucl. Phys. **B483** (1997) 267.
- [6] B. Kastening and X. Zhan, Phys. Rev. **D45** (1992) 3884.
- [7] K. Funakubo, S. Tao and F. Toyoda, hep-ph/0501052.
- [8] K. Funakubo and S. Tao, Prog. Theor. Phys. **113** (2005) 821.
- [9] T. Akiba, H. Kikuchi and T. Yanagida, Phys. Rev. **D38** (1988) 1937.